Geophysical Research Letters

RESEARCH LETTER
10.1029/2018GL079070

Ocean Circulation Reduces the Hadley Cell Response to Increased Greenhouse Gases

R. Chemke[1] and L. M. Polvani[1,2]

[1]Department of Applied Physics and Applied Mathematics, Columbia University, New York, NY, USA, [2]Department of Earth and Environmental Sciences and Lamont-Doherty Earth Observatory, Columbia University, Palisades, NY, USA

Key Points:
- Ocean circulation acts to reduce the Hadley cell response to increased greenhouse gases
- Convective heating is suppressed due to the reduced warming by ocean circulation
- The suppressed convective heating reduces the weakening and the expansion of the Hadley cell

Supporting Information:
- Supporting Information S1

Correspondence to:
R. Chemke,
rc3101@columbia.edu

Citation:
Chemke, R., & Polvani, L. M. (2018). Ocean circulation reduces the Hadley cell response to increased greenhouse gases. *Geophysical Research Letters*, *45*. https://doi.org/10.1029/2018GL079070

Received 3 JUN 2018
Accepted 11 AUG 2018
Accepted article online 22 AUG 2018

Abstract The Hadley cell (HC) plays an important role in setting the strength and position of the hydrological cycle. Climate projections show a weakening of the HC, together with widening of its vertical and meridional extents. These changes are projected to have profound global climatic impacts. Current theories for the HC response to increased greenhouse gases account only for atmospheric and oceanic thermodynamic changes and not for oceanic circulation changes. Here the effects of ocean circulation changes on the HC response to increased greenhouse gases are examined by comparing fully coupled and slab ocean model configurations. By reducing the warming of both the sea surface and the atmosphere, changes in ocean circulation reduce the HC response to increased CO_2 concentrations. This reduced warming suppresses convective heating, which reduces the weakening of the HC and the stabilization at low latitudes, and thus also reduces the meridional (in the Southern Hemisphere) and vertical HC expansion.

Plain Language Summary Given the importance of tropical circulation in affecting low-latitude climate, it is crucial to understand the projected response of tropical circulation to anthropogenic emissions. To fully understand the tropical circulation response, one must account for the internal feedbacks between the different components of the climate system. Here we study the effect of changes in ocean circulation in response to increased greenhouse gases on the tropical circulation. We find that ocean circulation acts to reduce the projected response of tropical circulation to anthropogenic emissions. This emphasizes the importance in using models with ocean circulation, when studying the long-term atmospheric response to increased greenhouse gases.

1. Introduction

The position and strength of Earth's climate zones are mostly determined by the large-scale atmospheric circulation. For example, by converging moist and warm air into the deep tropics and forcing descent of dry cold air in the subtropics, the Hadley cell (HC) is partially responsible for separating the wet tropical from the dry subtropical regions. By the end of the 21st century, the HC is projected to weaken and extend both its vertical and meridional edges (Intergovernmental Panel on Climate Change, 2013; Kang et al., 2013; Vallis et al., 2015), which have important societal impacts in tropical and subtropical regions (Intergovernmental Panel on Climate Change, 2014).

Several theories have been suggested to explain the response of the HC to increased greenhouse gases (GHG) concentrations, which we briefly review: (i) Regarding the circulation's strength, changes in both upper troposphere radiative (e.g., Bony et al., 2013; Knutson & Manabe, 1995; Merlis, 2015) and convective (e.g., Held & Soden, 2006; Knutson & Manabe, 1995; Schneider et al., 2010) heating, as well as eddy fluxes (e.g., Levine & Schneider, 2011) have been proposed to explain the weakening of the HC. (ii) Regarding the HC's meridional width, it was found to follow the latitude where the angular momentum conserving flow becomes baroclinically unstable (Held, 2000). Under increased GHG, the stabilization of the subtropics and its associated reduction in baroclinicity were found to shift the HC edge poleward (Lu et al., 2008; Son et al., 2018). (iii) Regarding the circulation's height, from radiative considerations alone, the height of the tropical tropopause is expected to increase, due to both a reduction in the temperature lapse rate and an increase in surface temperature (Thuburn & Craig, 1997, 2000; Vallis et al., 2015).

In all above theories, atmospheric and oceanic thermodynamic changes were taken into account. However, since ocean circulation plays an important role in setting the properties of the HC (e.g., Clement, 2006),

changes in ocean circulation, which are absent in those theories, may also affect the HC response to increased GHG.

Since the sea surface serves as a lower boundary for the atmosphere, any effects of ocean circulation on the tropical atmosphere must go through changes in sea surface temperature (SST). Several studies found that changes in ocean heat fluxes, under different types of forcing, result in profound tropical atmospheric circulation changes. Interhemispheric heat transfer by ocean circulation was found to counteract the shift of the ITCZ under both the RCP8.5 forcing scenario (McFarlane & Frierson, 2017) and changes in high-latitude surface energy balance (Deser et al., 2015; Green & Marshall, 2017; Hawcroft et al., 2017; Tomas et al., 2016). In the context of the HC, Levine and Schneider (2011), using an idealized slab ocean model (SOM), argued that under increased optical thickness, the wind-driven oceanic tropical heat flux acts to moderate the widening and weakening of the HC.

The aim of this work is to understand the role of changes in ocean circulation in affecting the response of the HC to increased GHG. The use of a SOM in Levine and Schneider (2011) did not enable them to investigate and quantify the full effect of ocean circulation changes. Thus, here we compare the response of the HC to increased CO_2 concentrations in a fully coupled ocean-atmosphere model (FOM), to the response in the same model but with a slab ocean. Contrasting the FOM to the SOM allows isolating and quantifying the effect of ocean circulation on the HC.

2. Methods

Two configurations of the Community Climate System Model version 4 (Gent et al., 2011) are used in this study; one with an active full-depth ocean (FOM) and one with a SOM (see Bitz et al., 2012; Kay et al., 2012, for further details). Both configurations use the Community Atmosphere Model version 4, with horizontal resolution of 1.25° × 0.9° and 26 vertical layers. The FOM uses the Parallel Ocean Program version 2, with 1° horizontal resolution and 60 vertical layers. Unlike in the FOM, in the SOM the ocean component is reduced to a slab ocean, with a depth calculated from a control FOM run. The slab ocean lacks any dynamical processes and only exchanges heat and moisture with the lowest atmospheric level. A Q-flux is added to the slab ocean temperature equation for producing similar climatology as in the control FOM (Bitz et al., 2012). This Q-flux is the same in all runs described below.

Two sets of runs (presented in Kay et al., 2012) are analyzed for each configuration: a preindustrial run with 1,850 forcing and CO_2 concentrations of 284.7 ppmv and a $2\times CO_2$ run with an instantaneous doubling of CO_2 concentrations to 569.4 ppmv (throughout the paper, the difference between the $2 \times CO_2$ and preindustrial runs is denoted by δ). Since the same Q-flux is applied in the preindustrial and $2\times CO_2$ runs, the SOM does not account for changes in ocean circulation under $2\times CO_2$ (i.e., the Q-flux does not respond to $2\times CO_2$). Thus, by comparing the responses of the two configurations to $2\times CO_2$, the role of ocean circulation in affecting the HC can be isolated and examined (i.e., this is the only process that responds to the forcing and does not appear in both models). To ensure that the HC has equilibrated, 300- and 60-year runs were conducted in the FOM and SOM, respectively. Following Kay et al. (2012), the results represent the average over the last 10 years of each run. Taking 20-year averages does not change the qualitative results of the study but does decrease the signal-to-noise ratio, as it accounts parts of the transient response.

Similar to Kang et al. (2013), three HC metrics are examined in this study:

a. The HC width ($\phi_{\Psi 500}$), defined as latitude where the meridional mass stream function,

$$\Psi = \frac{2\pi a \cos\phi}{g}\int_0^p \bar{v}\,dp, \tag{1}$$

at 500 mb first changes sign poleward of the latitude of maximum stream function in each hemisphere; here a is Earth's radius, g is gravity, v is meridional velocity, p is pressure, and overbar represents zonal and time mean.

b. The HC strength (Ψ_{max}), defined as the maximum absolute value of Ψ at 500 mb, in each hemisphere.

c. The HC height (H), defined as the tropopause height averaged between the latitudes of Ψ_{max} in the Northern Hemisphere (NH) and Southern Hemisphere (SH). Following the World Meteorological Organization, the tropopause height is defined as the lowest level where the temperature lapse reaches 2 K/km.

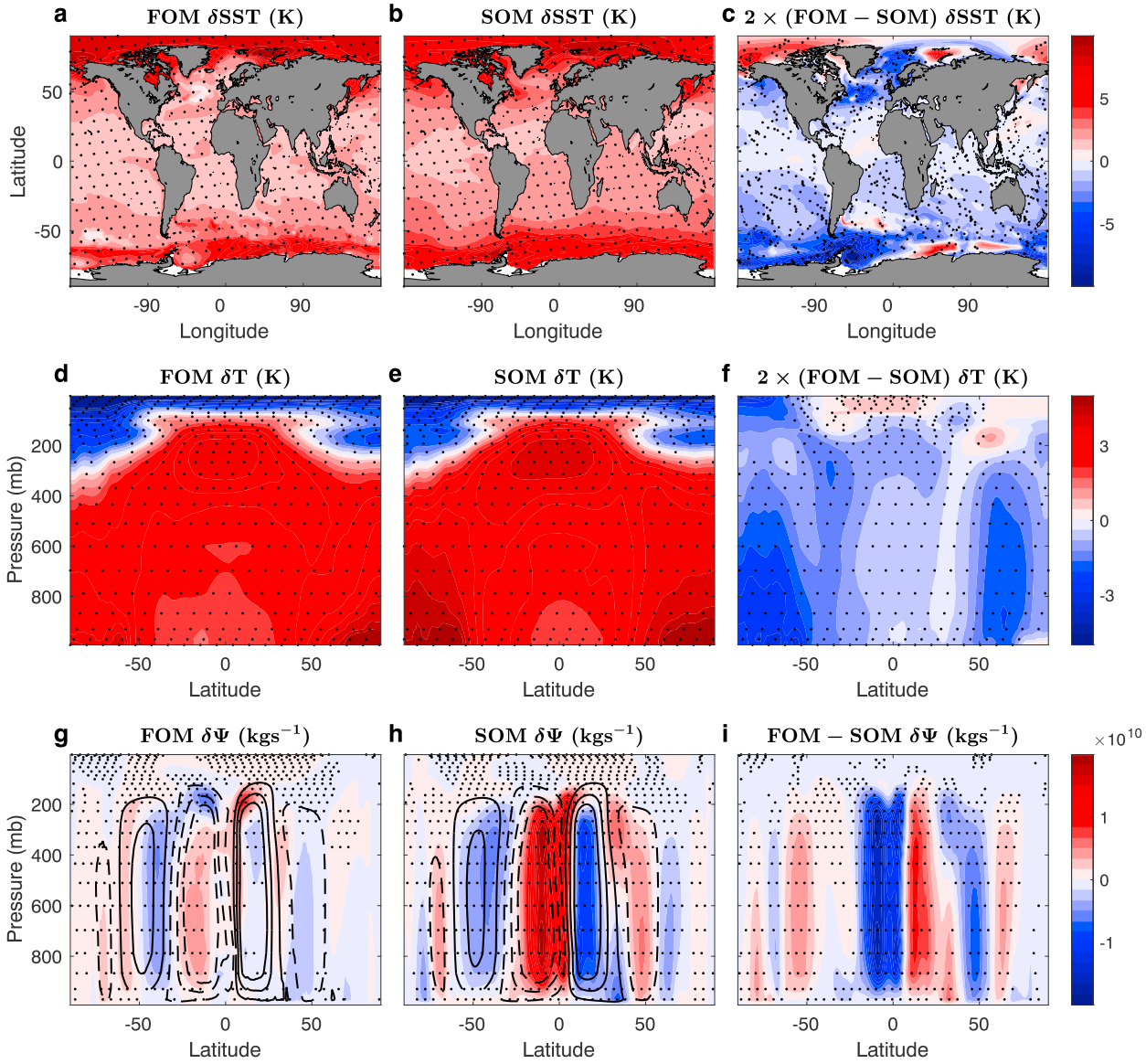

Figure 1. Mean (a–c) SST (K), (d–f) temperature (K), and (g–i) meridional mass stream function (kg/s) response to $2 \times CO_2$ in (a, d, g) the FOM, (b, e, h) SOM and (c, f, i) difference between FOM and SOM. Black contours in panels (g) and (h) show the stream function in the preindustrial run, where solid (dashed) contours represent clockwise circulation (counterclockwise). In panels (c) and (f) the difference in responses is multiplied by 2. The black dots show where the response is statistically significant at the 95% confidence level. SST = sea surface temperature; FOM = fully coupled ocean-atmosphere model; SOM = slab ocean model.

3. Results

As mentioned in section 1, any ocean circulation changes can only affect the atmosphere by modulating the SST. Therefore, we start by showing the SST response to $2 \times CO_2$ (Figures 1a–1c) in the FOM (panel a) and SOM (panel b). In both configurations, the SST shows the expected warming pattern of strong polar amplification. The difference in the responses between the FOM and SOM is shown in Figure 1c. Since the only difference between the FOM and SOM, which responds to $2 \times CO_2$, is the presence of ocean circulation in the former, the difference in the responses shown in Figure 1c represents the effects of ocean circulation on SST under $2 \times CO_2$. Ocean circulation acts to reduce the warming of the SST through most of the globe and more so at high latitudes than at low latitudes (e.g., Winton et al., 2013). This overall-reduced warming pattern is not confined to the surface but also extends into the atmosphere. Figures 1d–1f show the atmospheric temperature response, where both the FOM (panel d) and SOM (panel e) show the expected polar amplification along with a warming maximum of the upper tropics. As for the SST response, the ocean circulation acts to reduce the

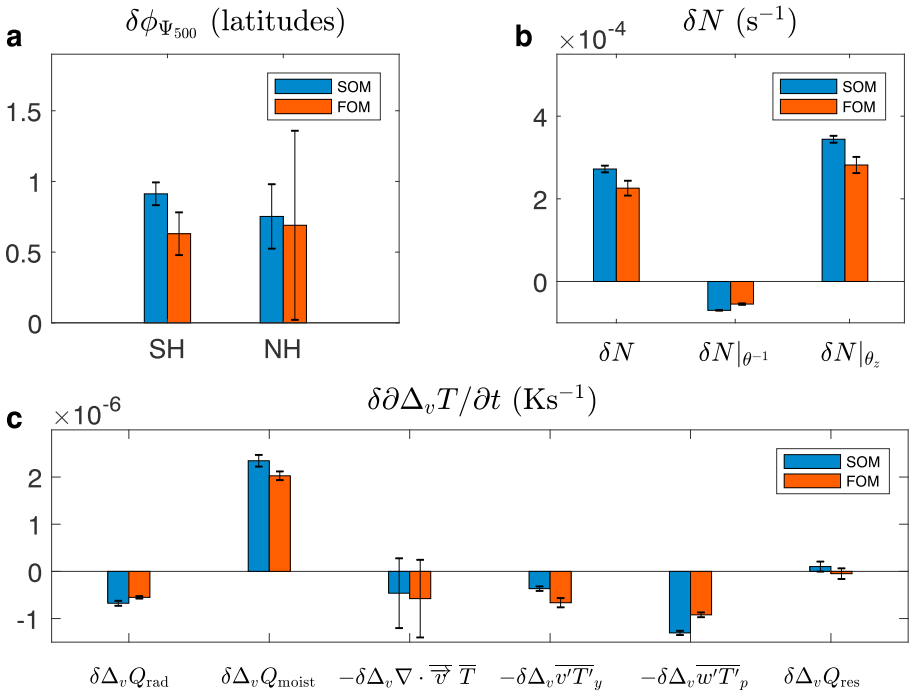

Figure 2. (a) The poleward shift of the Hadley cell edge ($\delta\phi_{\Psi 500}$, degrees latitudes, section 2) in the SH and NH. (b) SH subtropical static stability response (δN, s^{-1}), separated to changes in mean potential temperature ($\delta N|_{\theta^{-1}}$, s^{-1}) and to changes in the temperature lapse rate ($\delta N|_{\theta_z}$, s^{-1}). (c) The response of the SH subtropical vertical difference temperature tendency equation ($\delta\frac{\partial\Delta_v T}{\partial t}$,K/s, equation (3)); radiation ($\delta\Delta_v Q_{rad}$), convection ($\delta\Delta_v Q_{moist}$), mean temperature flux convergence ($-\delta\Delta_v\nabla\cdot\overline{\vec{v}}\,\overline{T}$), meridional ($-\delta\Delta_v\overline{v'T'_y}$) and vertical ($-\delta\Delta_v\overline{w'T'_p}$) eddy temperature flux convergence, and adiabatic and vertical diffusion ($\delta\Delta_v Q_{res}$). Blue and red bars show the SOM and FOM responses, respectively. Vertical error bars represent the 95% confidence interval over the analysis period. SH = Southern Hemisphere; NH = Northern Hemisphere; SOM = slab ocean model; FOM = fully coupled ocean-atmosphere model.

warming of most of the atmosphere and more at high latitudes than low latitudes (Figure 1f; e.g., Singh et al., 2017).

Because the atmospheric flow is driven by temperature gradients, the above temperature changes are expected to affect the atmospheric circulation. Figures 1g–1i show the meridional mass stream function (Ψ) response to $2\times CO_2$, where solid (dashed) black contours show the clockwise (counterclockwise) circulation in the preindustrial run. In both FOM (panel g) and SOM (panel h) the HC weakens under $2\times CO_2$, as seen by the red (blue) colors on dashed (solid) contours in the SH (NH) HC. This weakening is stronger in the SOM, indicating that the ocean circulation acts to reduce the weakening of the HC, as evidenced by the stronger blue (red) colors southward (northward) of the equator in Figure 1i, which shows the difference in the streamfunction responses. To elucidate and quantify the effect of ocean circulation on the three HC metrics (strength, width, and height), we now examine each metric in detail separately.

3.1. The HC Width

In the SH, the widening of the HC ($\delta\phi_{\Psi 500}$) under $2\times CO_2$ is 30% larger in the SOM (0.91°, blue bar in Figure 2a) than in the FOM (0.63°, red bar in Figure 2a). Thus, the ocean circulation acts to reduce the widening of the SH HC. In the NH, however, we find only a minor difference in $\delta\phi_{\Psi 500}$ between the SOM and FOM. Since the effect of ocean circulation on $\phi_{\Psi 500}$ is robust only in the SH, we next analyze the widening of the HC in the SH alone.

As discussed in section 1, under increased GHG the stabilization of the subtropics (the increase in static stability) is responsible for the poleward shift of the HC (e.g., Lu et al., 2008; Son et al., 2018). The subtropical (averaged between 30°S–40°S and 400–800 mb) static stability, $N=\left(\frac{g}{\theta}\frac{\partial\theta}{\partial z}\right)^{\frac{1}{2}}$ (where θ is potential temperature and z is height), indeed shows a larger increase in the SOM than in the FOM (δN, Figure 2b), in agreement with a larger HC expansion in the SOM than in the FOM. This shows that ocean circulation acts to reduce the stabilization of the subtropics under $2\times CO_2$. Further decomposing the response of N,

$$\delta N = g^{\frac{1}{2}} \left(\frac{\partial \theta}{\partial z}\right)^{\frac{1}{2}} \delta \left(\frac{1}{\theta}\right)^{\frac{1}{2}} + g^{\frac{1}{2}} \left(\frac{1}{\theta}\right)^{\frac{1}{2}} \delta \left(\frac{\partial \theta}{\partial z}\right)^{\frac{1}{2}} \quad (2)$$

to changes due to mean potential temperature ($\delta N|_{\theta^{-1}}$, first term on the right-hand side of equation (2)) and changes due to temperature lapse rate ($\delta N|_{\theta_z}$, second term on the right-hand side of equation (2)), shows that the difference in stabilization between the SOM and FOM is largely due to changes in the temperature lapse rate (Figure 2b).

In order to isolate which physical processes make the ocean circulation affect the subtropical temperature lapse rate under $2 \times CO_2$, the different terms of the temperature equation are examined. By subtracting the lower-level temperature equation from the upper-level temperature equation, a temperature equation for the vertical temperature difference ($\Delta_v T$) can be written, for simplicity in Cartesian coordinates, as follows:

$$\frac{\partial \Delta_v T}{\partial t} = \Delta_v Q_{\text{rad}} + \Delta_v Q_{\text{moist}} - \Delta_v \nabla \cdot \overline{\vec{v}T} - \Delta_v \frac{\partial \overline{v'T'}}{\partial y} - \Delta_v \frac{\partial \overline{w'T'}}{\partial p} + \Delta_v Q_{\text{res}}, \quad (3)$$

where Δ_v is a vertical difference between upper (300–500 mb) and lower (600–800 mb) levels, T is temperature, t is time, Q_{rad} and Q_{moist} are diabatic heating due to radiation and convection, respectively, $\vec{v}$ is wind vector in the meridional and vertical directions, $\overline{\vec{v}T}$ is mean meridional and vertical heat fluxes, $\overline{v'T'}$ and $\overline{w'T'}$ are meridional and vertical eddy heat fluxes, respectively, where w is vertical velocity, and Q_{res} includes adiabatic heating ($\frac{wTR}{pc_p}$, where $R = 287$ J·kg·$^{-1}$·K^{-1} is the gas constant of dry air and $c_p = 1004$ J·kg·$^{-1}$·K^{-1} is the specific heat of air) and vertical diffusion. At steady state, the left-hand side of equation (3) is zero: hence, a positive value of the response of each of the terms to $2 \times CO_2$ indicates that it acts to stabilize the atmosphere (decrease the lapse rate) and a negative value to destabilize it (increase the lapse rate).

In both SOM and FOM, the only term that acts to stabilize the subtropics with $2 \times CO_2$ is Q_{moist} ($\delta \Delta_v Q_{\text{moist}}$, Figure 2c). Because more water vapor is available for condensation in a warmer climate (owing to the Clausius-Clapeyron relation), convective heating increases and warms the upper levels. This decreases the temperature lapse rate, stabilizes the subtropics, and, following the Held (2000) theory, pushes $\phi_{\Psi 500}$ poleward. Convective heating (Q_{moist}) also contributes to the difference between the SOM and FOM. Since the ocean circulation acts to reduce the warming of both the surface and atmosphere (Figures 1c and 1f), less water vapor is available for condensation in the FOM, leading to a weaker stabilization by convective heating, which reduces the poleward expansion of the HC.

Another term that contributes to the different lapse rate response between the SOM and FOM is the eddy meridional heat flux convergence ($-\delta \Delta_v \overline{v'T'_y}$, Figure 2c). The eddy meridional heat flux convergence acts to destabilize the subtropics in both configurations, as it transports less heat poleward, thus warming the lower levels at low latitudes. Since this effect is larger in the FOM than the SOM, the eddy meridional heat flux convergence also contributes to the more stabilized subtropics in the SOM. All other terms in equation (3) cannot explain the stronger stratification in the FOM than in the SOM.

3.2. The HC Strength

While ocean circulation affects $\phi_{\Psi 500}$ mostly in the SH (Figure 2a), it affects the weakening of HC in both hemispheres (Figures 3a and 3d): it is also of a much greater amplitude. In the SH, the weakening of the HC strength to $2 \times CO_2$ ($\delta \Psi_{\text{max}}$) is 75% larger in the SOM (1.38×10^{10} kg/s, blue bar in Figure 3a) than in the FOM (3.33×10^9 kg/s, red bar in Figure 3a). Similarly, in the NH, the weakening of Ψ_{max} to $2 \times CO_2$ is 90% larger in the SOM (9.08×10^9 kg/s, blue bar in Figure 3d) than in the FOM (9.4×10^8 kg/s, red bar in Figure 3d). Thus, similar to Levine and Schneider (2011), the ocean circulation acts to reduce the weakening of the HC under $2 \times CO_2$.

To better understand the difference in HC weakening between the two configurations, an equation for the overturning stream function is now analyzed. Assuming a quasi-geostrophic approximation and using thermal wind balance, an equation for the overturning stream function (the Kuo-Eliassen equation; Kuo, 1956) can be written as follows (see section 14.5.5 in Peixoto & Oort, 1992):

$$f^2 \frac{\partial^2 \psi}{\partial p^2} + S^2 \frac{\partial^2 \psi}{\partial y^2} = \frac{R}{p} \left(\frac{\partial Q_{\text{diab}}}{\partial y} - \frac{\partial^2 \overline{v'T'}}{\partial y^2} \right) + f \left(\frac{\partial^2 \overline{u'v'}}{\partial p \partial y} - \frac{\partial X}{\partial p} \right), \quad (4)$$

where f is the Coriolis parameter, $S^2 = -\frac{1}{\rho\theta} \frac{\partial \theta}{\partial p}$ is static stability, ρ is density, Q_{diab} is diabatic heating, $\overline{u'v'}$ is eddy momentum fluxes, and X is zonal friction. Equation (4) is numerically solved by applying an iterative method

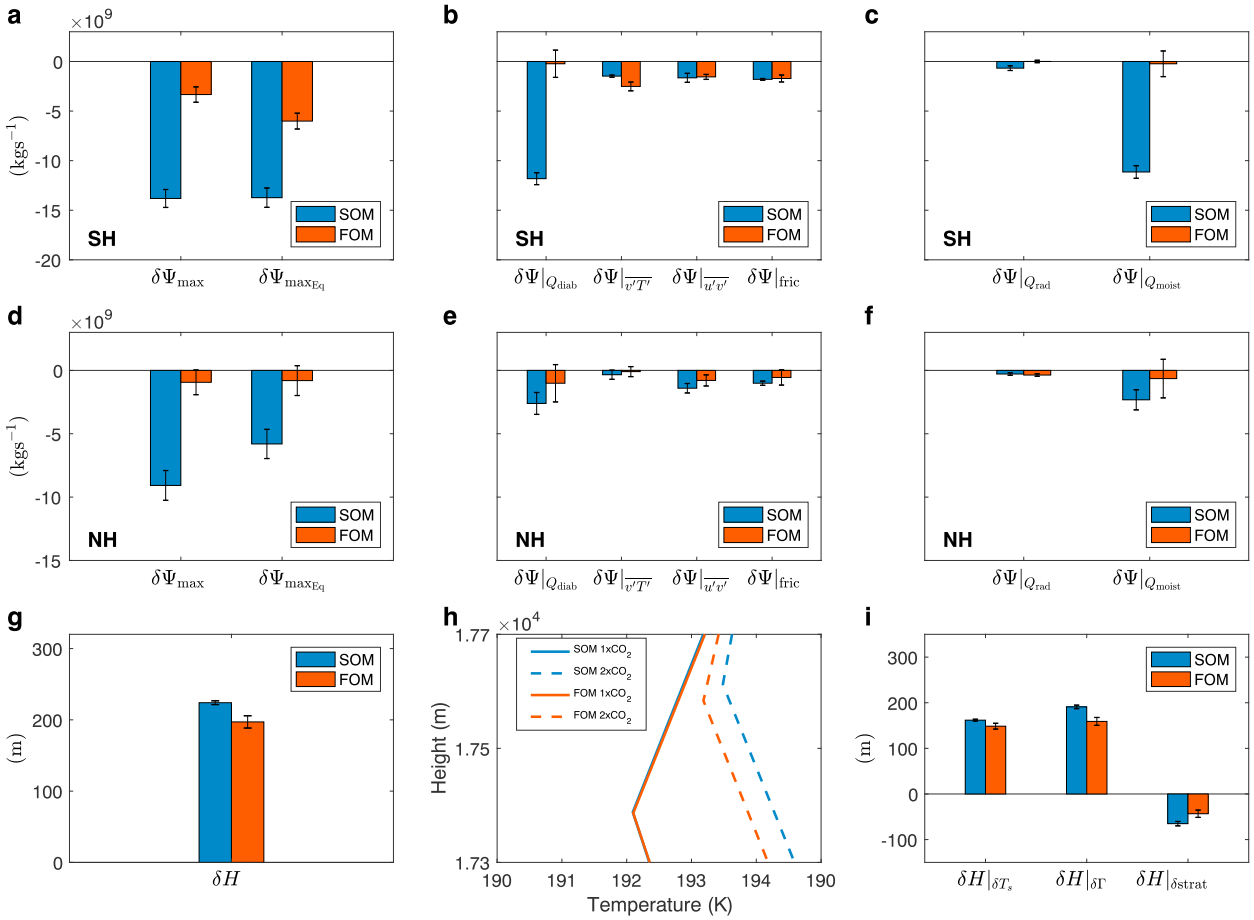

Figure 3. Hadley cell strength (a–c for SH and d–f for NH) and height (g–i) responses to $2 \times CO_2$. (a, d) The response of the Hadley cell strength (kg/s) based on equations (1) (Ψ_{max}) and (4) ($\Psi_{max_{Eq}}$). (b, e) The response of the different terms in equation (4) (kg/s); diabatic ($\delta\Psi|_{Q_{diab}}$), eddy heat fluxes ($\delta\Psi|_{\overline{v'T'}}$), eddy momentum fluxes ($\delta\Psi|_{\overline{u'v'}}$), and zonal friction ($\delta\Psi|_{fric}$). (c, f) The response of the diabatic term in equation (4) separated to contributions from radiative heating ($\delta\Psi|_{Q_{rad}}$) and convective heating ($\delta\Psi|_{Q_{moist}}$). (g) The tropical tropopause height response (δH, m, section 2). (h) The vertical profile of tropical temperatures in the SOM (blue lines) and FOM (red lines) for the preindustrial (solid lines) and $2 \times CO_2$ (dashed lines) runs. (i) The relative contributions of surface temperature ($\delta H|_{\delta T_s}$), tropospheric lapse rate ($\delta H|_{\delta\Gamma}$) and stratospheric temperature and lapse rate ($\delta H|_{\delta strat}$) to the tropopause height response (equation (6)). Blue and red bars show the SOM and FOM responses, respectively. Vertical error bars represent the 95% confidence interval over the analysis period. SH = Southern Hemisphere; NH = Northern Hemisphere; SOM = slab ocean model; FOM = fully coupled ocean-atmosphere model.

(successive overrelaxation) to its finite difference approximation (in spherical coordinates, supporting information). Since ψ vanishes at the boundaries, in the above elliptic equation ψ is proportional to the negative of the right-hand side. Thus, in the deep tropics Q_{diab} decreases with latitude and acts to drive the HC, while in the low subtropics it is the increase of the eddy fluxes with latitude and height. Surface zonal friction also acts to strengthen the HC.

Similar to the Ψ_{max} response to $2 \times CO_2$, the solution of equation (4) (its maximum value at 500 mb) shows a greater weakening in the SOM than in the FOM in both hemispheres (Figures 3a and 3d). Solving equation (4) for each of the right-hand side terms separately yields their relative contribution in weakening the HC (evaluated at 500 mb and at the latitude of maximum weakening). While changes in diabatic heating are mostly important for the weakening of the HC in the SOM in both hemispheres (Figures 3b and 3e; e.g., Bony et al., 2013; Held & Soden, 2006; Knutson & Manabe, 1995; Merlis, 2015; Su et al., 2014), in the FOM, eddy fluxes also contribute to the weakening of the HC in both hemispheres (e.g., Levine & Schneider, 2011). Diabatic heating also accounts for most of the difference between the SOM and FOM in both hemispheres. Further decomposing the changes in diabatic heating into radiative and convective heating shows that most of the difference between the SOM and FOM comes from changes in convective heating (Figures 3c and 3f). This again shows that the different HC responses in the two configurations come from the tendency of the ocean circulation to reduce changes in convective heating by reducing the warming of the surface and atmosphere.

3.3. The HC Height

The response of the HC height to $2 \times CO_2$ (δH) is 12% larger in the SOM (224 m, blue bar in Figure 3h) than in the FOM (197 m, red bar in Figure 3h). Changes in H could be due to both changes in mean temperature and changes in the lapse rate (e.g., Thuburn & Craig, 2000; Vallis et al., 2015). Figure 3h shows the tropical (averaged between the latitudes of Ψ_{max} in the SH and NH) temperature vertical structure around the tropopause height. The SOM (blue lines) shows a larger increase than the FOM (red lines) in both upper tropospheric and lower stratospheric temperatures. Since these increases have opposite effects on H and in order to quantify the relative contributions of the mean temperature and lapse rate to changes in H, an equation for H is examined.

Assuming constant lapse rates with height in the troposphere and stratosphere, the stratospheric temperature (T_{strat}) can be written as follows:

$$T_{strat}(z) = T_s + \Gamma_{trop} H + \Gamma_{strat}(z - H), \tag{5}$$

where T_s is the surface temperature and Γ_{trop} and Γ_{strat} are the tropospheric and stratospheric lapse rates, respectively. Isolating the tropopause height (H) in equation (5) yields an equation for changes in tropopause height (δH),

$$\delta H = -\frac{\delta T_s}{\Gamma_{trop} - \Gamma_{strat}} - \frac{H \delta \Gamma_{trop}}{\Gamma_{trop} - \Gamma_{strat}} + \frac{\delta T_{strat} - \delta \Gamma_{strat}(z - H)}{\Gamma_{trop} - \Gamma_{strat}}, \tag{6}$$

where the first term on the right-hand side of equation (6) accounts for changes in surface temperature, the second term for changes in tropospheric lapse rate, and the third term for changes in both stratospheric temperature and lapse rate. Equation (6) is similar to equation 9 in Vallis et al. (2015) but generalized to a nonisothermal stratosphere, so that changes in stratospheric temperature under $2 \times CO_2$ may also affect H.

In both SOM and FOM an increase in surface temperature ($\delta H|_{\delta T_s}$) and a decrease in the tropospheric lapse rate ($\delta H|_{\delta \Gamma}$) act to increase H (Figure 3i). Changes in stratospheric temperature and lapse rate ($\delta H|_{\delta strat}$), on the other hand, act to decrease H. Most of the difference in the response of H between the SOM and FOM is due to a stronger decrease in the tropospheric lapse in the SOM ($\delta H|_{\delta \Gamma}$). As discussed in section 3.1, the tendency of ocean circulation to reduce the warming of both the surface and atmosphere reduces the amount of upper troposphere convective heating (the amount of available saturated water vapor for condensation is reduced), which yields a smaller decrease in the lapse rate and thus in H as well with $2 \times CO_2$.

3.4. Changes in Ocean Circulation

Finally, we ask: which changes in ocean circulation are responsible for reducing the warming in the tropics and subtropics and for reducing the response of the HC to $2 \times CO_2$? To answer this question, the zonal mean oceanic mixed-layer temperature tendency equation is now examined (e.g., Dong et al., 2007), which can be written as follows:

$$\rho c_p h \frac{\partial \overline{SST}}{\partial t} = SHF - \rho c_p h \overline{(v_g + v_\tau)} \frac{\partial \overline{SST}}{\partial y} - \rho c_p \overline{w_\tau \Delta_v T_{ml}} - \rho c_p h \overline{Q_{res}}, \tag{7}$$

where $\rho = 1,027$ kg/m^3 is ocean density; $c_p = 3,985$ J·kg·$^{-1}$·K^{-1} is seawater-specific heat capacity; h is mixed-layer depth; SHF is net air-sea heat fluxes; $v_g = \frac{g}{f}\frac{\partial SSH}{\partial x}$ is meridional geostrophic flow, where SSH is the sea surface height; $hv_\tau = -\frac{\tau_x}{\rho f}$ is the meridional Ekman transport, where τ_x is zonal wind stress; w_τ is vertical Ekman velocity; $\Delta_v T_{ml}$ is the temperature difference between the top and bottom of the mixed layer; and Q_{res} includes vertical turbulent mixing and entrainment at the bottom of the mixed layer. At steady state the left-hand side of equation (7) is zero, and Q_{res} is estimated as the residual.

The response of the different terms in equation (7) to $2 \times CO_2$ is plotted in Figure 4. In the tropics (averaged between the ITCZ, defined as the latitude where Ψ changes sign at 500 mb between the latitudes of Ψ_{max} in the SH and NH, and $\phi_{\Psi 500}$), in both hemispheres most of the reduced warming is due to a reduction in meridional heat flux by the Ekman flow ($\delta v_\tau SST_y$, Figure 4a). This reduced warming is responsible for reducing both the weakening of the HC (section 3.2) and the increase in H (section 3.3). These effects cause the ocean circulation to act as a negative feedback on the HC strength response to $2 \times CO_2$. As the HC weakens (Figure 3a), the reduced tropical easterlies (which are in balance with the equatorward meridional flow) exert less stress on the ocean surface, which results in less oceanic heat transfer from the equator into the tropics (Figures 1c and 4a). The reduced warming of the tropics acts to reduce the weakening of the HC, through convective heating (Figure 3c). This is in agreement with Levine and Schneider (2011), who found that the meridional heat flux by

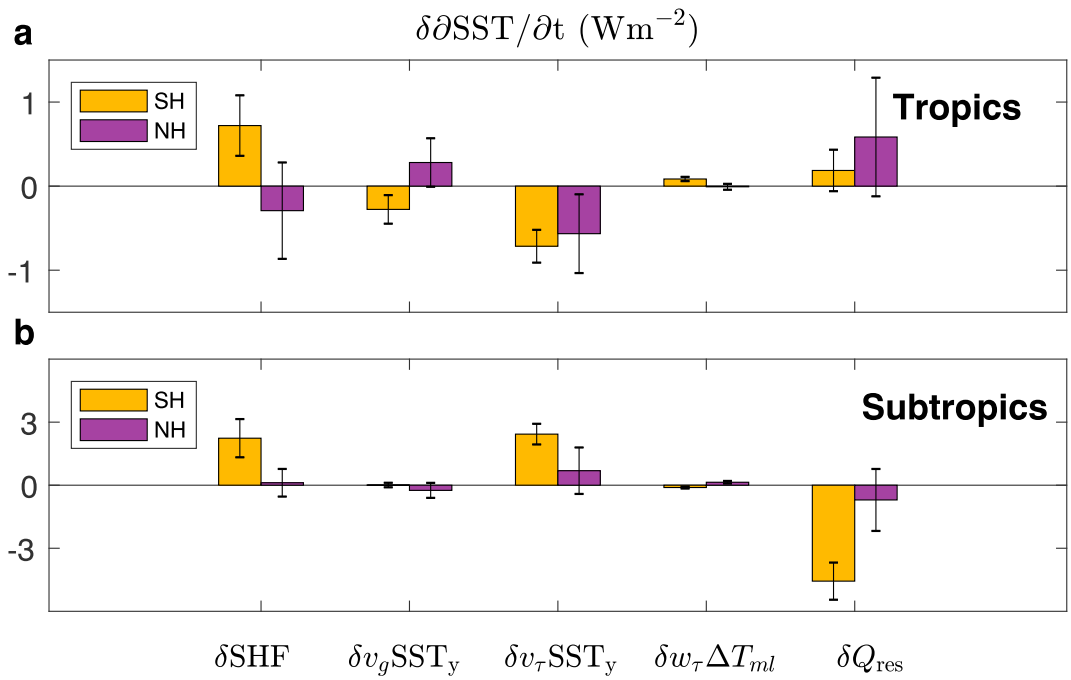

Figure 4. The response of the mixed-layer temperature equation (W/m^2, equation (7) in the FOM to 2 × CO_2 in the (a) tropics and (b) subtropics; air-sea heat fluxes (δSHF), meridional advection by geostrophic flow ($\delta v_g \mathrm{SST}_y$), meridional advection by Ekman flow ($\delta v_\tau \mathrm{SST}_y$), vertical advection by ekman flow ($\delta w_\tau \Delta T_{\mathrm{ml}}$), and vertical heat transfers by turbulent mixing and entrainment at the mixed-layer base (δQ_{res}). Yellow and purple bars show the response in the SH and NH, respectively. Vertical error bars represent the 95% confidence interval over the analysis period. FOM = fully coupled ocean-atmosphere model; SST = sea surface temperature; SH = Southern Hemisphere; NH = Northern Hemisphere.

Ekman transport results in a more moderate decrease of the HC strength with increased optical thickness. In the subtropics (averaged between 30°S–40°S), the reduced warming occurs due to changes in vertical heat transfers (δQ_{res}, Figure 4b), which reduces the widening of the HC (section 3.1). The weakened expansion due to changes in Ekman heat transport, reported in Levine and Schneider (2011), does not play an important role in the FOM.

4. Conclusions

The importance of the HC in affecting the hydrological cycle and Earth's climate is the main reason for the extensive study of its projected response to increased GHG. The HC is projected to weaken and to expand, both meridionally and vertically. While most theories for these changes account for atmospheric and oceanic thermodynamic responses to increased GHG, they do not account for changes in ocean circulation. Unlike previous studies which only accounted for the effect of the ocean using a SOM (e.g., Levine & Schneider, 2011), we have here elucidated and quantified the full effects of changes in ocean, including changes in the circulation, on the HC response to 2 × CO_2. This is done by comparing a FOM with a slab ocean version.

The ocean circulation is found to reduce the weakening and expansion of the HC. In the tropics, the weakening of the HC under 2 × CO_2 weakens the meridional oceanic Ekman transport, which reduces tropical warming. This reduced warming suppresses convective heating at high levels that limits the weakening of the circulation. Thus, the ocean circulation has a negative feedback on the HC strength. The suppressed convective heating also reduces the increase of the tropical tropopause height, as it diminishes the decrease of the temperature lapse rate.

In the SH subtropics, reduction in oceanic vertical mixing reduces the warming of the surface and the atmosphere as well. This again suppresses convective heating that limits the decrease of the temperature lapse rate. Since the HC width is controlled by the static stability in the subtropics, the reduced stabilization by ocean circulation limits the poleward expansion of the HC.

The importance of ocean circulation in modulating the atmospheric response to increased GHG is not limited to the tropics. Ocean circulation was found to play an important role in affecting both Southern Ocean (e.g., Armour et al., 2016; Lu & Zhao, 2012; Singh et al., 2017) and Arctic (e.g., Deser et al., 2016; Singh et al., 2017; Winton, 2003) climate responses to increased GHG. Our findings add to this literature with further evidence for the importance of using coupled GCMs, where ocean circulation is taken into an account, when studying the atmospheric response to increased GHG.

Acknowledgments
We thank Jeniffer Kay and Gokhan Danabasoglu for providing the data of the simulations. The research was supported by the NOAA Climate and Global Change Postdoctoral Fellowship Program, administered by UCAR's Cooperative Programs for the Advancement of Earth System Science (CPAESS). L. M. P. is funded, in part, from a grant of the National Science Foundation to Columbia University. The data used here are listed in the text and references.

References

Armour, K. C., Marshall, J., Scott, J. R., Donohoe, A., & Newsom, E. R. (2016). Southern Ocean warming delayed by circumpolar upwelling and equatorward transport. *Nature Geoscience*, *9*, 549–554.

Bitz, C. M., Shell, K. M., Gent, P. R., Bailey, D. A., Danabasoglu, G., Armour, K. C., et al. (2012). Climate sensitivity of the community climate system model, version 4. *Journal of Climate*, *25*, 3053–3070.

Bony, S., Bellon, G., Klocke, D., Sherwood, S., Fermepin, S., & Denvil, S. (2013). Robust direct effect of carbon dioxide on tropical circulation and regional precipitation. *Nature Geoscience*, *6*, 447–451.

Clement, A. C. (2006). The role of the ocean in the seasonal cycle of the Hadley circulation. *Journal of the Atmospheric Sciences*, *63*, 3351–3365.

Deser, C., Sun, L., Tomas, R. A., & Screen, J. (2016). Does ocean coupling matter for the northern extratropical response to projected Arctic sea ice loss?. *Geophysical Research Letters*, *43*, 2149–2157. https://doi.org/10.1002/2016GL067792

Deser, C., Tomas, R. A., & Sun, L. (2015). The role of ocean-atmosphere coupling in the zonal-mean atmospheric response to Arctic sea ice loss. *Journal of Climate*, *28*, 2168–2186.

Dong, S., Gille, S. T., & Sprintall, J. (2007). An assessment of the Southern Ocean mixed layer heat budget. *Journal of Climate*, *20*, 4425–4442.

Gent, P. R., Danabasoglu, G., Donner, L. J., Holland, M. M., Hunke, E. C., Jayne, S. R., et al. (2011). The community climate system model version 4. *Journal of Climate*, *24*, 4973–4991.

Green, B., & Marshall, J. (2017). Coupling of trade winds with ocean circulation damps ITCZ shifts. *Journal of Climate*, *30*, 4395–4411.

Hawcroft, M., Haywood, J. M., Collins, M., Jones, A., Jones, A. C., & Stephens, G. (2017). Southern Ocean albedo, inter-hemispheric energy transports and the double ITCZ: Global impacts of biases in a coupled model. *Climate Dynamics*, *48*, 2279–2295.

Held, I. M. (2000). The general circulation of the atmosphere, *Program in Geophysical Fluid Dynamics*. Woods Hole, MA: Woods Hole Oceanographic Institute. Retrieved from http://www.whoi.edu

Held, I. M., & Soden, B. J. (2006). Robust responses of the hydrological cycle to global warming. *Journal of Climate*, *19*, 5686–5699.

Intergovernmental Panel on Climate Change (2013). Summary of policymakers. In T. F. Stocker, et al. (Eds.), *Climate change 2013: The physical basis* (pp. 1–29). New York: Cambridge University Press.

Intergovernmental Panel on Climate Change (2014). Summary of policymakers. In C. B. Feild, et al. (Eds.), *Climate change 2014: Impacts, adaptation, and vulnerability* (pp. 1–32). New York: Cambridge University Press.

Kang, S. M., Deser, C., & Polvani, L. M. (2013). Uncertainty in climate change projections of the Hadley circulation: The role of internal variability. *Journal of Climate*, *26*, 7541–7554.

Kay, J. E., Holland, M. M., Bitz, C. M., Blanchard-Wrigglesworth, E., Gettelman, A., Conley, A., & Bailey, D. (2012). The influence of local feedbacks and northward heat transport on the equilibrium arctic climate response to increased greenhouse gas forcing. *Journal of Climate*, *25*, 5433–5450.

Knutson, T. R., & Manabe, S. (1995). Time-mean response over the tropical pacific to increased $C0_2$ in a coupled ocean-atmosphere model. *Journal of Climate*, *8*, 2181–2199.

Kuo, H.-L. (1956). Forced and free meridional circulations in the atmosphere. *Journal of the Atmospheric Sciences*, *13*, 561–568.

Levine, X. J., & Schneider, T. (2011). Response of the Hadley circulation to climate change in an aquaplanet GCM coupled to a simple representation of ocean heat transport. *Journal of the Atmospheric Sciences*, *68*, 769–783.

Lu, J., Chen, G., & Frierson, D. M. W. (2008). Response of the zonal mean atmospheric circulation to El Niño versus global warming. *Journal of Climate*, *21*, 5835–5851.

Lu, J., & Zhao, B. (2012). The role of oceanic feedback in the climate response to doubling CO_2. *Journal of Climate*, *25*, 7544–7563.

McFarlane, A. A., & Frierson, D. M. W. (2017). The role of ocean fluxes and radiative forcings in determining tropical rainfall shifts in RCP8.5 simulations. *Geophysical Research Letters*, *44*, 8656–8664.

Merlis, T. M. (2015). Direct weakening of tropical circulations from masked CO_2 radiative forcing. *Proceedings of the National Academy of Sciences of the United States of America*, *112*(43), 13,167–13,171.

Peixoto, J. P., & Oort, A. H. (1992). *Physics of climate*. New York: American Institute of Physics.

Schneider, T., O'Gorman, P. A., & Levine, X. J. (2010). Water vapor and the dynamics of climate change. *Reviews of Geophysics*, *48*, RG3001.

Singh, H. A., Rasch, P. J., & Rose, B. E. J. (2017). Increased ocean heat convergence into the high latitudes with CO_2 doubling enhances polar-amplified warming. *Geophysical Research Letters*, *44*, 10,583–10,591. https://doi.org/10.1002/2017GL074561

Son, S.-W., Kim, S. Y, & Min, S. K (2018). Widening of the Hadley cell from last glacial maximum to future climate. *Journal of Climate*, *31*, 267–281.

Su, H., Jiang, J. H., Zhai, C., Shen, T. J., Neelin, J. D., Stephens, G. L., & Yung, Y. L. (2014). Weakening and strengthening structures in the Hadley Circulation change under global warming and implications for cloud response and climate sensitivity. *Journal of Geophysical Research: Atmospheres*, *119*, 5787–5805. https://doi.org/10.1002/2014JD021642

Thuburn, J., & Craig, G. C. (1997). GCM tests of theories for the height of the tropopause. *Journal of the Atmospheric Sciences*, *54*, 869–882.

Thuburn, J., & Craig, G. C. (2000). Stratospheric influence on tropopause height: The radiative constraint. *Journal of the Atmospheric Sciences*, *57*, 17–28.

Tomas, R. A., Deser, C., & Sun, L. (2016). The role of ocean heat transport in the global climate response to projected Arctic sea ice loss. *Journal of Climate*, *29*, 6841–6859.

Vallis, G. K., Zurita-Gotor, P., Cairns, C., & Kidston, J. (2015). Response of the large-scale structure of the atmosphere to global warming. *Quarterly Journal of the Royal Meteorological Society*, *141*, 1479–1501.

Winton, M. (2003). On the climatic impact of ocean circulation. *Journal of Climate*, *16*, 2875–2889.

Winton, M., Griffes, S. M., Samuels, B. L., Sarmiento, J. L., & Frölicher, T. L. (2013). Connecting Changing Ocean Circulation with Changing Climate. *Journal of Climate*, *26*, 2268–2278.